



Optics Letters

Tailored supercontinuum generation using genetic algorithm optimized Fourier domain pulse shaping

MATHILDE HARY,^{1,2}  LAURI SALMELA,¹  PIOTR RYCZKOWSKI,¹  FRANCESCA GALLAZZI,¹ 
JOHN M. DUDLEY,²  AND GOËRY GENTY^{1,*} 

¹Photonics Laboratory, Tampere University, FI-33104 Tampere, Finland

²Université de Franche-Comté, Institut FEMTO-ST, CNRS UMR 6174, 25000 Besançon, France

*goery.genty@tuni.fi

Received 3 April 2023; revised 14 June 2023; accepted 14 June 2023; posted 15 June 2023; published 17 July 2023

We report the generation of a spectrally tailored supercontinuum using Fourier-domain pulse shaping of femtosecond pulses injected into a highly nonlinear fiber controlled by a genetic algorithm. User-selectable spectral enhancement is demonstrated over the 1550–2000-nm wavelength range, with the ability to both select a channel with target central wavelength and bandwidth in the range of 1–5 nm. The spectral enhancement factor relative to unshaped input pulses is typically ~5–20 in the range 1550–1800 nm and increases for longer wavelengths, exceeding a factor of 160 around 2000 nm. We also demonstrate results where the genetic algorithm is applied to the enhancement of up to four spectral channels simultaneously.

Published by Optica Publishing Group under the terms of the [Creative Commons Attribution 4.0 License](https://creativecommons.org/licenses/by/4.0/). Further distribution of this work must maintain attribution to the author(s) and the published article's title, journal citation, and DOI.

<https://doi.org/10.1364/OL.492064>

A supercontinuum is a versatile light source that has revolutionized many applications such as imaging, spectroscopy, and sensing [1,2]. The dynamics of supercontinuum generation is highly nonlinear and complex, especially in the anomalous dispersion regime where the resulting spectral features are associated with ejected soliton pulses, dispersive waves generation, soliton self-frequency shift, and spectral interference [1]. Although it is now routine to generate supercontinuum spectra with very broad bandwidths, obtaining a desired spectral coverage with a large fraction of intensity in particular wavelength bands is more challenging, often requiring time-consuming trial and error experiments as well as computationally demanding simulations. In this context, attempts have been made to exploit the soliton self-frequency shift to optimize the spectral intensity at a particular wavelength by manipulating the input peak power of injected pulses [3]. However, this approach is typically restricted to intensity optimization at one wavelength and it also imposes limitations on the injected power to ensure fundamental soliton propagation.

Machine learning is showing great promise in enabling “smart” control of light sources [4–6], and techniques such as

genetic algorithms (GAs) and neural networks have been applied to actively control the complex dynamics and output characteristics of pulses from fiber lasers [7–13], extra-cavity pulse compression [14], and controlled spectral broadening in planar waveguides induced by multi-pulse sequences [15]. In this paper, we apply a genetic algorithm to the systematic optimization of supercontinuum generation in a highly nonlinear fiber (HLNF), focusing in particular on enhancing the spectral intensity in narrow spectral channels with bandwidths of 1 nm and 5 nm, selected arbitrarily over the wavelength range of 1550–2000 nm. Our results could be of significant interest to optimize supercontinuum for diverse application such as fluorescence microscopy [16] or frequency metrology [17].

Our approach is based on computer-controlled Fourier-domain spectral shaping to adjust the phase of femtosecond pulses injected into a highly nonlinear fiber. Specifically, a genetic algorithm optimizes the spectral phase of the input pulses so as to maximize the spectral intensity in one or more desired spectral channels. Note that this approach is similar to coherent combining in the spatial domain and which can be used, e.g., for the optimization of beam splitters [18,19]. For a single target spectral channel, we quantify the spectral enhancement resulting from the optimization as a function of the desired central wavelength, and show that the technique works best for longer wavelengths exceeding ~1850 nm with enhancement factors in the range of 10–160. We also show that the algorithm can be adapted for multi-channel enhancement with the simultaneous optimization of the spectral density in three and four channels. We also describe the evolution properties of the algorithm which shows rapid convergence to the desired target regime in ~20 generations for single-channel optimization, and after ~50 generations for the multi-channel case. These results provide a further demonstration of the power of machine learning techniques in harnessing complex dynamical processes for particular applications in photonics.

Figure 1 shows our experimental setup. The pump laser is a fiber laser (NKT Photonics ORIGAMI) generating pulses at 1559.3 nm with 40.9-MHz repetition rate. The maximum laser output power is 93 mW and the pulse energy is 2.2 nJ. The pulses have a 200-fs duration (FWHM) and a bandwidth of 14 nm such that their time-bandwidth product is $\Delta\tau\Delta\nu = 0.321$, close to the transform limit. The pulses then pass through a

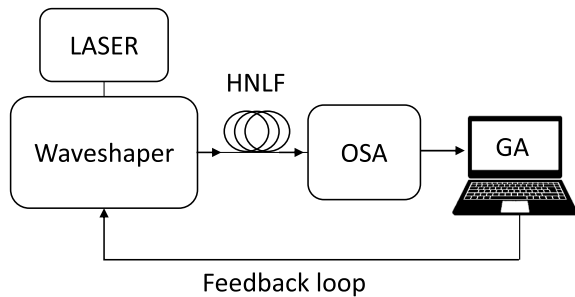


Fig. 1. Schematic of the pulse shaping apparatuses and the feedback loop from the genetic algorithm to the spatial light modulator (SLM) placed in the Fourier plane of the 4-f system. Light is collected after the pulse shaper and focused into a highly nonlinear fiber (HNLf). The fiber output is coupled into an optical spectrum analyzer (OSA, Yokogawa AQ6376) and the spectral intensity characteristics are optimized by a genetic algorithm which controls the spectral phase applied to the SLM.

standard 4-f Fourier-domain pulse shaper system (see Supplement 1 for details) and focused into 5 m of highly nonlinear fiber (Thorlabs HN1550-P). The coupling efficiency is 40%. The fiber has nonlinear parameter $\gamma = 10.8 \times 10^{-3} \text{ W}^{-1} \text{ m}^{-1}$ and near-zero group velocity dispersion at the pump laser wavelength $D = -1 \pm 1 \text{ ps}/(\text{nm km})$. For ease of handling and coupling, the highly nonlinear fiber was spliced to 15-cm standard fiber (SMF-28) patchcords at each end. Note that each splice loss is less than 1.2 dB, with nonlinearity and dispersion parameters of $\gamma = 1.2 \times 10^{-3} \text{ W}^{-1} \text{ m}^{-1}$ and $D = 16 \text{ ps}/(\text{nm km})$, respectively.

The spectral phase imposed by the SLM is controlled by a genetic algorithm to enhance in target spectral channels the intensity of the supercontinuum generated in the highly nonlinear fiber. Note that evolutionary algorithms have been previously applied for the optimization of femtosecond and nanosecond laser pulses [16,20–29] and here, our approach is specifically adapted to the optimization of the supercontinuum characteristics.

The algorithm evolves a population of 50 individuals, each individual specified by the five parameters of the system (genes). The SLM phase function applied in the Fourier plane is given by $\phi_{\text{SLM}}(\omega) = c_2(\omega - \omega)^2 + c_3(\omega - \omega_0)^3 + c_4(\omega - \omega_0)^4$, where the three coefficients (genes) c_2, c_3, c_4 quantify the spectral phase contributions up to fourth order (quartic), and the central frequency of the phase pattern ω_0 constitutes a fourth gene. In addition, a fifth gene can be optimized to control the overall system throughput and hence the input power injected into the fiber. This is achieved by applying a phase ramp to the SLM in the direction orthogonal to the grating dispersion and tilting the beam. The angular tilt decreases the light coupling efficiency to the fiber [30].

Starting from an input generation of randomly selected genes, we compute for each individual a fitness function [31]. In the case of single-channel optimization, this fitness function corresponds to the integrated spectral intensity around a specific target wavelength and over a specified bandwidth: $S = \int I(\lambda)d\lambda$. The individuals in the subsequent generation are then selected using standard techniques of elitism (5%), crossover (9%), and mutation (8%). This process evolves through multiple generations until convergence is reached and there is no significant further improvement. The “best” individual is then retained as

the algorithm output. Note that for speed of execution, the fitness function during the optimization steps for each individual is computed by scanning over a limited bandwidth of 30 nm around the target channel and the full spectrum is recorded only upon convergence. The implementation was done using the Global Optimization toolbox from MATLAB and optimization takes typically 25 minutes per wavelength optimization.

Figures 2(a) and 2(b) show typical results targeting spectral optimization at 1900 nm and for target bandwidths of $\Delta\lambda = 1 \text{ nm}$ and $\Delta\lambda = 5 \text{ nm}$, respectively. More specifically, Figs. 2(a) and 2(b) plot in blue the HNLf output supercontinuum spectra without optimization (i.e., using only the unshaped pulses) and with GA optimization (red and purple). The insets show the optimized spectral phase profile. Corresponding temporal profiles are shown in Supplement 1. The GA-optimized results were obtained after 50 generations. When comparing Figs. 2(a) and 2(b), it is clear that, although the optimized spectra are different over the range 1500–1800 nm, the intensity characteristics around the target wavelength of 1900 nm are similar [with a spectrally broader feature in Fig. 2(b) as expected].

We repeated the optimization procedure above for target channels in the full range of 1550–2000 nm scanned in increments of 50 nm (and again for bandwidths of $\Delta\lambda = 1 \text{ nm}$ and $\Delta\lambda = 5 \text{ nm}$). It is convenient to quantify the optimization results here by defining a spectral intensity enhancement factor $\eta = S_f/S_i$, where S_f and S_i are the optimized and unoptimized spectral intensities (i.e., with no phase applied and $c_2 = c_3 = c_4 = 0$) integrated over the target bandwidths, respectively. Figure 2(c) plots the enhancement factor as a function of target channel for bandwidths of $\Delta\lambda = 1 \text{ nm}$ (red) and $\Delta\lambda = 5 \text{ nm}$ (blue). The algorithm yields excellent performance with greater than 20× enhancement above 1800 nm. The results for both bandwidths show a similar trend. The improved performance at longer wavelengths is attributed to the fact that the particular spectral feature that is being optimized here is a distinct Raman-shifted soliton pulse which is separated from the more modulated spectral features closer to the pump.

For multi-wavelength optimization, we need to define a more complex fitness function that favors the enhancement of spectral characteristics at a number of different wavelengths simultaneously (see Supplement 1 for details). Figures 3(a) and 3(b) show results of the optimization for three (1550 nm, 1750 nm, and 1850 nm) and four channels (1600 nm, 1700 nm, 1800 nm, and 1850 nm) simultaneously. Note that the wavelengths were selected arbitrarily for illustration purposes. The GA evolution reveals that the regime of convergence is reached rapidly in less than 20 generations when only a single channel is optimized, although the precise evolution for any particular experiment does depend on the initial genes that are selected randomly. For multi-channels optimization, between 30 to 40 generations were found to be typical to enter into the optimal regime. See Supplement 1 for a more detailed study.

The particular choice of pump laser (central wavelength, duration) and nonlinear fiber characteristics (dispersion, nonlinearity, and length) significantly influences the supercontinuum generating dynamics and determine the extent of spectral tuning that can be achieved. It is then important to bear in mind that achieving an arbitrary user-defined supercontinuum spectrum may not be possible for a fixed number of user-controlled parameters. Yet, the experiments reported here show that the strong dependence of the supercontinuum features on the input phase parameters applied before propagation into a highly nonlinear

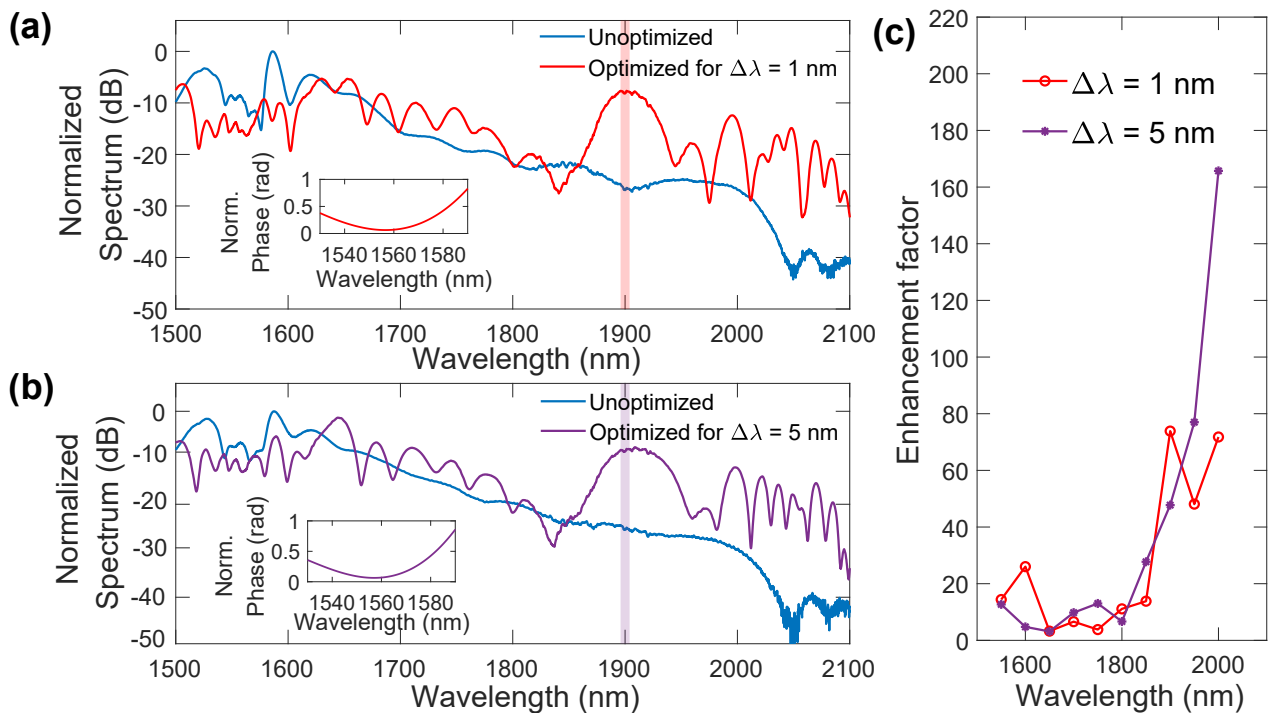


Fig. 2. (a),(b) Plot of the HNLf output spectra in logarithmic scale without optimization (i.e., generated by unshaped pulses with $c_2 = c_3 = c_4 = 0$) in blue, and the HNLf output spectra with GA optimization for bandwidth of $\Delta\lambda = 1$ nm and $\Delta\lambda = 5$ nm in red and purple, respectively. The spectra are normalized with respect to the maximum spectral intensity recorded over the measurement series. The insets show the optimized phase profile. Corresponding coefficients (see text) are $c_2 = 5.81 \cdot 10^{-27} \text{s}^{-2}$, $c_3 = -6.6 \cdot 10^{-41} \text{s}^{-3}$, $c_4 = -2.43 \cdot 10^{-56} \text{s}^{-4}$ in panel (a) and $c_2 = 5.88 \cdot 10^{-27} \text{s}^{-2}$, $c_3 = -8.359 \cdot 10^{-41} \text{s}^{-3}$, $c_4 = -1.159 \cdot 10^{-55} \text{s}^{-4}$ in panel (b). (c) Spectral intensity enhancement factor versus wavelength for single-channel optimization and bandwidths of $\Delta\lambda = 1$ nm (red) and $\Delta\lambda = 5$ nm (purple).

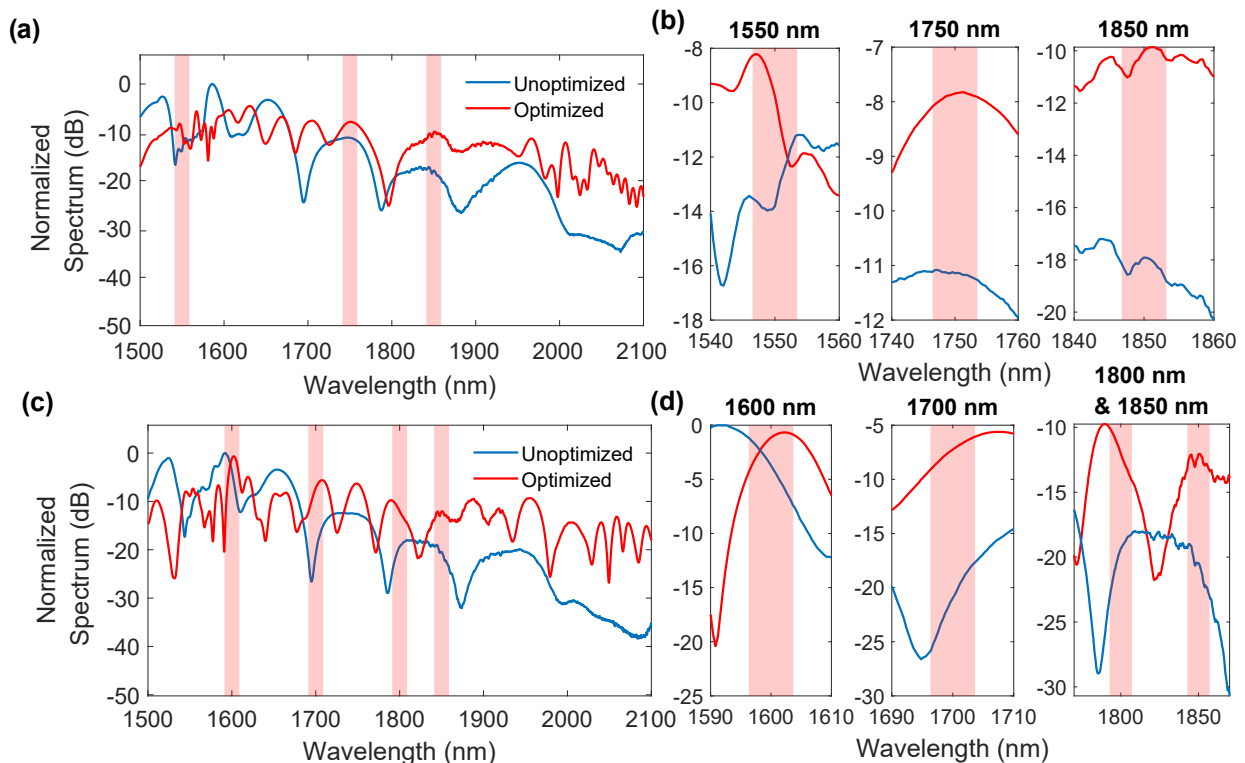


Fig. 3. Optimization of multiple spectral channels simultaneously: (a) at 1550 nm, 1750 nm and 1850 nm; (c) at 1600 nm, 1700 nm, 1800 nm, and 1850 nm. (b),(d) Zoomed regions of the spectrum. Both figures show the spectrum before (blue) and after optimization by the GA (red). Note that the spectrum before optimization can slightly change due to fluctuations in the pump laser power. The red rectangles indicate the position of the optimized spectral channels.

fiber can be efficiently exploited for significant spectral intensity enhancement at an arbitrary single channel and for multiple combinations of different channels with a genetic algorithm in less than 30 minutes. Of course, the optimization of specific combinations of spectral channels may yield varying degrees of enhancement, due to the underlying generating supercontinuum dynamics. Our results here were demonstrated over the 1550–2000-nm range, limited by the optical spectrum analyzer, but one can in principle extend the wavelength range.

A significant benefit of the genetic algorithm is that it can compensate for small variations (of the order of a few % in the input pulse parameters due to, e.g., laser drift) through the mutation coefficient, which introduces random coefficients at each generation. However, in the case of more significant changes such as, e.g., misalignment, the algorithm needs to be re-run to effectively adapt to the modified input conditions. Finally, although here we have used a genetic algorithm showing excellent performance, previous studies have shown that other search algorithms could also be employed [15,18]. Our results open up novel perspectives for light sources with on-demand spectra tailored to specific applications.

Funding. French Investissements d’Avenir Programme; Agence Nationale de la Recherche (ANR-15-IDEX-0003, ANR-17-EURE-0002, ANR-20-CE30-0004); Academy of Finland (318082, 320165, 333949).

Disclosures. The authors declare no competing interests.

Data availability. Data are available from the corresponding author upon reasonable request. All codes used in the manuscript were the standard GA suite within the MATLAB Global Optimization toolbox.

Supplemental document. See Supplement 1 for supporting content.

REFERENCES

- J. Dudley and J. Taylor, *Supercontinuum Generation in Optical Fibers* (Cambridge University Press, 2010).
- A. Labruyère, A. Tonello, V. Couderc, G. Huss, and P. Leproux, *Opt. Fiber Technol.* **18**, 375 (2012).
- E. R. Andresen, V. Birkedal, J. Thøgersen, and S. R. Keiding, *Opt. Lett.* **31**, 1328 (2006).
- G. Genty, L. Salmela, J. M. Dudley, D. Brunner, A. Kokhanovskiy, S. Kobtsev, and S. K. Turitsyn, *Nat. Photonics* **15**, 91 (2021).
- M. Närhi, L. Salmela, J. Toivonen, C. Billet, J. M. Dudley, and G. Genty, *Nat. Commun.* **9**, 4923 (2018).
- L. Salmela, N. Tsipinakis, A. Foi, C. Billet, J. M. Dudley, and G. Genty, *Nat. Mach. Intell.* **3**, 344 (2021).
- J. N. Kutz, X. Fu, and S. Brunton, *Advanced Photonics*, Barcelona, Spain (July 2014), paper NTu4A.7.
- M. Tianprateep, J. Tada, T. Yamazaki, and F. Kannari, *Jpn. J. Appl. Phys.* **43**, 8059 (2004).
- W. Q. Zhang, A. V. Shahraam, and T. M. Monro, *Opt. Express* **17**, 19311 (2009).
- F. R. Arteaga-Sierra, C. Milián, I. Torres-Gómez, M. Torres-Cisneros, G. Moltó, and A. Ferrando, *Opt. Express* **22**, 23686 (2014).
- S. Boscolo and C. Finot, *Opt. Laser Technol.* **131**, 106439 (2020).
- B. S. Vikram, R. Prakash, S. K. Selvaraja, and V. R. Supradeepa, *Opt. Express* **28**, 11215 (2020).
- D. Lorenc, D. Velic, A. N. Markevitch, and R. J. Levis, *Opt. Commun.* **276**, 288 (2007).
- Y. Shen, Y. Wang, H. Chen, K. Luan, M. Tao, and J. Si, *Sci. Rep.* **7**, 14913 (2017).
- B. Wetzel, M. Kues, P. Roztocky, C. Reimer, P.-L. Godin, M. Rowley, B. E. Little, S. T. Chu, E. A. Viktorov, D. J. Moss, A. Pasquazi, M. Peccianti, and R. Morandotti, *Nat. Commun.* **9**, 4884 (2018).
- J. Tada, T. Kono, A. Suda, H. Mizuno, A. Miyawaki, K. Midorikawa, and F. Kannari, *Appl. Opt.* **46**, 3023 (2007).
- K. F. Lee, A. Rolland, P. Li, J. Jiang, and M. E. Fermann, *Opt. Express* **30**, 427 (2022).
- H. Dammann and K. Görtler, *Opt. Commun.* **3**, 312 (1971).
- N. Streibl, *J. Mod. Opt.* **36**, 1559 (1989).
- C. A. Farfan, J. Epstein, and D. B. Turner, *Opt. Lett.* **43**, 5166 (2018).
- A. Efimov, M. D. Moores, N. M. Beach, J. L. Krause, and D. H. Reitze, *Opt. Lett.* **23**, 1915 (1998).
- T. Baumert, T. Brixner, V. Seyfried, M. Strehle, and G. Gerber, *Appl. Phys. B: Lasers Opt.* **65**, 779 (1997).
- M. Song, S. Han, J. Park, H. Choi, S. Kim, T. T. Tran, H. D. Kim, and M. Song, *Opt. Express* **29**, 12001 (2021).
- K. Kashiwagi, H. Ishizu, Y. Kodama, and T. Kurokawa, *Opt. Express* **21**, 3001 (2013).
- U. Andral, R. S. Fodil, F. Amrani, F. Billard, E. Hertz, and P. Grelu, *Optica* **2**, 275 (2015).
- L. Michaeli and A. Bahabad, *J. Opt.* **20**, 055501 (2018).
- F. G. Omenetto, B. P. Luce, and A. J. Taylor, *J. Opt. Soc. Am. B* **16**, 2005 (1999).
- C. Lapre, F. Meng, M. Hary, C. Finot, G. Genty, and J. M. Dudley, *Sci. Rep.* **13**, 1865 (2023).
- L. Salmela, M. Hary, M. Mabed, A. Foi, J. M. Dudley, and G. Genty, *Opt. Lett.* **47**, 802 (2022).
- E. Frumker and Y. Silberberg, *J. Opt. Soc. Am. B* **24**, 2940 (2007).
- R. L. Haupt and S. E. Haupt, *Practical Genetic Algorithms* (John Wiley and Sons Inc. Publication, 2004).